

WHAT GRAVITATIONAL SIGNALS SAY ABOUT THE STRUCTURE AND THE EVOLUTION OF ASTROPHYSICAL SOURCES

V. FERRARI

*Dipartimento di Fisica "G.Marconi", Università di Roma "La Sapienza"
and Sezione INFN ROMA1, p.le A. Moro 5, I-00185 Roma, Italy
E-mail: valeria@roma1.infn.it*

Gravitational waves transport very detailed information on the structure and evolution of astrophysical sources. For instance a binary system in the early stages of its evolution emits a wavetrain at specific frequencies that depend on the characteristics of the orbital motion; as the orbit shrinks and circularize, due to radiation reaction effects, the orbiting bodies get closer and tidally interact. This interaction may result in the excitation of the proper modes of oscillation of the stars, and in the emission of gravitational signals that carry information on the mode frequencies, and consequently on the equation of state in the stellar interior. These phenomena may occur either in solar type stars with orbiting planets and in compact binaries, and in this lecture we will discuss different approaches that can be used to study these processes in the framework of General Relativity.

In recent years, major progresses have been done in the construction of large ground-based interferometers, which will make accessible to observations a large frequency region, ranging from a few Hz to a few kHz: TAMA has already performed some observational runs, reaching a sensitivity that would enable to detect the coalescence of a neutron star-neutron (NS-NS) binary system occurring in our Galaxy with a signal to noise ratio higher than 30, and VIRGO, LIGO and GEO600, are almost completely assembled and within the end of the year 2002 are expected to start scientific runs¹. Resonant bar detectors, ALLEGRO, AURIGA, EXPLORER, NAUTILUS, NIOBE, have been operational since many years, and are sensitive to a small frequency region of about 10-20 Hz, centered at ~ 1 kHz. As an example, Explorer and Nautilus would be able to detect, with signal to noise ratio equal to 1, a burst of gravitational waves of amplitude $h \sim 4 \cdot 10^{-19}$, which would correspond to a mass of a few units in $10^{-3} M_{\odot}$ transforming into gravitational waves at the center of our Galaxy². And finally, the space-based interferometer LISA, which is expected to fly in about a decade, will enlarge the observational window to the low frequency region $10^{-4} \text{ Hz} \lesssim \nu \lesssim 10^{-1} \text{ Hz}$.

Many are the astrophysical sources that, according to the theory of General Relativity, emit gravitational waves in the frequency region spanned by these detectors, and in this review I will discuss the characteristic properties of the signals emitted by some of the more interesting sources, and show how

to compute them. The detectability of a signal depends also on the *event rate*, namely on how many events per year occur in the volume accessible to observations, and on the *detection rate*, which depends on the response of each detector to a specific source; how these rates are determined is, of course, a very important issue, but a discussion of these problems is beyond the scope of this review, which will be focussed on the information that the gravitational signals carry on the structure (either geometrical or internal) of the source, on its motion, and on physical processes that may occur in some particular situations, like the resonant excitation of the stellar modes.

In Sec. I, I will shortly describe the quadrupole formalism, which is the easiest method to estimate gravitational fluxes and waveforms, and I will discuss its domain of applicability. In Sec. II and III, the quadrupole formalism will be applied to rotating neutron stars and to binary systems far from coalescence, respectively. In Sec. IV the resonant excitation of the g-modes in extrasolar planetary systems will be considered in the framework of a perturbative approach, and in Sec. V the gravitational emission of coalescing binary systems will be studied.

1 The quadrupole formalism

The quadrupole formalism is one of the most powerful tools to estimate the amount of radiation emitted by a dynamically evolving system. It is based on the assumptions that the gravitational field is weak, so that gravitational interaction do not dominate, and that the velocities of the bodies involved in the problem are much smaller than the speed of light; as a consequence, the spacetime metric can be written as the metric of the flat spacetime, $\eta_{\mu\nu}$, plus a small perturbation

$$g_{\mu\nu} = \eta_{\mu\nu} + h_{\mu\nu}, \quad |h_{\mu\nu}| \ll 1,$$

and the Einstein equations can be linearized and solved. By a suitable choice of the gauge, the perturbation $h_{\mu\nu}$ is found to satisfy a wave equation, and to propagate in vacuum at the speed of light; its amplitude is shown to depend only on the time variation of the energy density of the source, $\rho(t, \mathbf{x})$, as follows

$$\begin{cases} h^{ij} = \frac{2G}{c^4} \frac{e^{i\omega \frac{z}{c}}}{r} \left[\frac{1}{c^2} \frac{\partial^2}{\partial t^2} q^{ij} \right] \\ h^{\mu 0} = 0, \quad \mu = 0, 3 \end{cases} \quad , \quad q^{ij} = \int_V \rho(t, \mathbf{x}) c^2 x^i x^j dV, \quad (1)$$

where q^{ij} is the quadrupole moment, and the integral extends over the source volume.

An interesting point to stress: the assumption

$$v \ll c \quad \rightarrow \quad \Omega R \ll c,$$

where R is the source extension, implies that the region where the source is confined must be small compared to the wavelength of the emitted radiation, $\lambda_{GW} = \frac{2\pi c}{\Omega}$. When this constraint is not verified, the quadrupole approach is no longer applicable. For instance, the binary system PSR 1931+16³, whose emission properties will be described in some more detail in the next section, is composed of two neutron stars with masses $M_1 \sim M_2 \sim 1.4M_\odot$, moving on an eccentric orbit of diameter $D \sim 13.8 \cdot 10^{10} \text{ cm}$; due to the orbital motion it emits gravitational waves at some specific frequencies, and the highest spectral line is at $\nu_{GW} \sim 10^{-4} \text{ Hz}$. It follows that

$$\lambda_{GW} = \frac{c}{\nu_{GW}} \sim 10^{14} \text{ cm}, \quad \lambda_{GW} \gg D,$$

and the quadrupole constraint is satisfied. But if we want to describe a pulsating neutron star, since the frequency of the fundamental mode of oscillation ranges within $\sim 2 - 3 \text{ kHz}$, depending on the equation of state (EOS), and since the typical diameter of a NS is $D \sim 20 \text{ km}$,

$$\lambda_{GW} = \frac{c}{\nu_{GW}} \sim \frac{3 \cdot 10^{10} \text{ cm/s}}{2 - 3 \cdot 10^3 \text{ Hz}} \sim 10^7 \text{ cm}, \quad \text{i.e.} \quad \lambda_{GW} \sim D,$$

and the quadrupole formalism cannot be applied. To study these problems, alternative and more sophisticated approaches have to be used as we shall see in Sec. 4.

2 Rotating neutron stars

As a first application of the quadrupole formalism, we shall consider the case of rotating neutron stars. Neutron stars can radiate their positive rotational energy essentially in two ways. If the star is triaxial, it has a time varying quadrupole moment and, according to Eq. (1), emits gravitational waves at twice the rotation frequency, and with an amplitude which can be parametrized in the following way⁴

$$h \sim 4.2 \times 10^{-24} \left(\frac{ms}{P}\right)^2 \left(\frac{r}{10 \text{ kpc}}\right)^{-1} \frac{I}{10^{45} \text{ g cm}^2} \left(\frac{\epsilon}{10^{-6}}\right) \quad (2)$$

where $I = 10^{45} \text{ g cm}^2$, is the typical value of the moment of inertia of a neutron star, P is the rotation period, and ϵ is the oblateness of the star, here

given in units of 10^{-6} . These waves could be detected, for instance, by VIRGO with one year of integration, if the amplitude of the signal were of the order of $h \sim 10^{-26}$; this means that neutron stars outside our Galaxy would practically be undetectable. In addition, much depends on the value of the oblateness, and several studies have tried to set limits on its possible range of variation. Gourghoulon and Bonazzola made a first attempt to set constraints on ϵ using observational data⁵. They considered a number of pulsars, and assuming that the observed slowing down of the period is entirely due to the emission of GW, gave an estimate of ϵ . They found $\epsilon \in \sim [10^{-2}, 10^{-9}]$, but of course this can only be an upper bound, since we know that rotational energy is dissipated in pulsars also by other mechanisms, like the electromagnetic emission and/or the acceleration of charged particles in the magnetosphere. Further studies on this problem⁶ established that if the triaxial shape is due to strains in the crust of the neutron star, the oblateness could be $\epsilon \lesssim 10^{-7} \left(\frac{\sigma}{10^{-2}}\right)$, where σ is the strain needed to break the crust, but its value is quite uncertain; for instance $\sigma \in [10^{-2}, 10^{-1}]$ according to⁷, and $\sigma \in [10^{-4}, 10^{-3}]$ according to⁸. A time dependent quadrupole moment can also be due to a precession of the star's angular velocity around the symmetry axes. In this case the radiation is emitted at a frequency $\nu_{prec} = \frac{1}{2\pi}(\omega_{rot} + \omega_{prec}) \simeq \nu_{rot}$, but the amplitude of the precessional contribution depends on a further parameter, the “wobble-angle” between the rotation and the symmetry axes, which is largely unknown. From the above discussion, we can conclude that unless astronomical observations will set more stringent constraints on the oblateness and on the wobble-angle of rotating neutron stars, it is difficult, at present, to say whether the radiation emitted by rotating neutron stars will be detectable in the near future.

It is worth mentioning that the detection of gravitational waves depends on many cooperating factors; indeed a signal is detectable if its frequency is in the range of the detector's bandwidth, if its amplitude is high enough to be extracted from the noise by a suitable filtering technique, and, last but not least, if the computing resources are sufficient to execute this operation. For instance, in the case of rotating neutron stars, the estimated number of sources in the Galaxy is $\sim 10^9$, of which, ~ 1000 are observed as pulsars, and 5 are at a distance smaller than 200pc; thus, at least the number of possible sources is encouraging; for some of them we have some further information, like the location in sky and the spin-down rate. However, we do not know the oblateness and since the star is certainly in relative motion with respect to the detector, the filters to be used to extract the signal from noise must contain the Doppler correction; thus, to detect signals from stars of unknown position and characteristics, we should divide the sky in patches as small as possible,

and search for possible sources by using filters with different parameters, and this is extremely expensive!

3 Binary systems far from coalescence: the quadrupole approach

The dynamical evolution of a binary system is affected by the emission of gravitational waves; due to the energy loss the orbit contracts, the orbital velocity increases and the system emits more gravitational energy. The process of inspiralling proceeds faster and faster as the system shrinks and finally the two bodies coalesce and merge. In this section we shall consider only systems that are far from coalescence. Since the two stars are far apart, their internal structure is not affected by the tidal interaction, and it is possible to treat them as two pointlike masses revolving around their common center of mass. In this case the time varying quadrupole moment is entirely due to the orbital motion of the two masses, and the emitted waveform is easily calculated by the quadrupole formula (1).

In 1975, Hulse and Taylor applied the quadrupole formalism to predict the slowing down of the period of the binary pulsar PSR 1913+16³. They found $\frac{dP}{dt} = -2.4 \cdot 10^{-12}$, in excellent agreement with the observed value, $\frac{dP}{dt} = -(2.3 \pm 0.22) \cdot 10^{-12}$, thus providing the first indirect evidence of the existence of gravitational waves. But now the question is: can these waves be detected directly? The quadrupole formula shows that when the orbit is circular the radiation is emitted at twice the keplerian orbital frequency

$$\nu_k = \frac{1}{P} = \frac{1}{2\pi} \left(\frac{GM}{R^3} \right)^{1/2}, \quad (3)$$

where $M = M_1 + M_2$ is the total mass of the system; if it is eccentric, as in the case of PSR 1913+16,^a waves will be emitted at frequencies multiple of ν_k (in this case, R must be replaced in Eq. (3) by the semi-major axis), and the number of equally spaced spectral lines will increase with the eccentricity⁹. It is convenient to introduce a characteristic amplitude which can be compared to the detectors sensitivity as follows¹⁰

$$h_c(n\nu_k, r) = \sqrt{\frac{2}{3}} \left[\langle \tilde{h}_{\theta\theta}^{(n)} \rangle^2 + \langle \tilde{h}_{\theta\phi}^{(n)} \rangle^2 \right]^{1/2}, \quad (4)$$

^aPSR 1913+16 is composed of two very compact stars, with masses $M_1 = 1.4411 M_\odot$ and $M_2 = 1.3874 M_\odot$, revolving around their center of mass with an eccentric orbit ($e = 0.617139$), and keplerian frequency $\nu_k = (\omega_k/2\pi) = 3.583 \cdot 10^{-5}$ Hz. The system is at a distance $D = 5$ kpc from Earth.

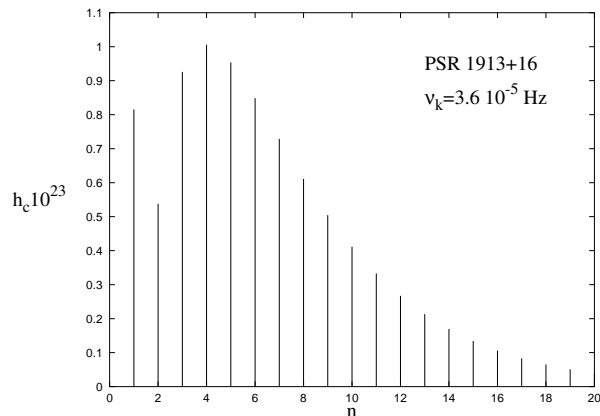


Figure 1: The characteristic amplitude of the wave emitted by PSR 1913+16 is plotted versus the harmonic index n . The spectral lines are emitted at frequencies multiple of ν_k .

where $\langle \tilde{h}_{\theta\theta}^{(n)} \rangle^2$ and $\langle \tilde{h}_{\theta\phi}^{(n)} \rangle^2$, are the square of the n -th Fourier component of the two independent polarizations, averaged over the solid angle

$$\langle \tilde{h}_{\theta\theta}^{(n)} \rangle^2 = \frac{1}{4\pi} \int d\Omega |h_{\theta\theta}(n\nu_k, r, \theta, \phi)|^2, \quad \langle \tilde{h}_{\theta\phi}^{(n)} \rangle^2 = \frac{1}{4\pi} \int d\Omega |h_{\theta\phi}(n\nu_k, r, \theta, \phi)|^2,$$

and the factor $\sqrt{2/3}$ takes into account the average over orientation. In the previous expressions, the waveforms have been expanded in Fourier series $h(t) = \sum_{n=-\infty}^{+\infty} h(n\omega_k) e^{-2in\pi t/P}$, and $h(n\omega_k) = \frac{1}{P} \int_0^P h(t) e^{+2in\pi t/P} dt$, where $\omega_k = 2\pi\nu_k$.

The characteristic amplitude h_c emitted by PSR 1913+16 is shown in figure 1 as a function of the harmonic index n . The maximum occurs at $\nu_{max} = 1.44 \cdot 10^{-4} Hz$, and the amplitude of the corresponding line is $h_{c\ max} \sim 10^{-23}$.

Thus the emission of this system is in the bandwidth of the space-based interferometer LISA, but the expected sensitivity curve of this instrument shows that the signal is too low to be detectable even with five years of integration.

However, other interesting sources of radiation of this kind exist in our Galaxy. For instance, in a recent paper the gravitational emission of cataclysmic variables has been considered¹¹. These systems are semi-detached binaries of low mass and very short period, in which the primary star is an accreting degenerate white dwarf, and the secondary is usually a late type-star filling its Roche lobe and transferring matter on the companion. In table I the

Table 1: Cataclysmic variables with component masses m_1 and m_2 , gravitational wave frequency ν_{GW} , and gravitational wave amplitude h_c .

| name | $m_1(M_\odot)$ | $m_2(M_\odot)$ | ν_{GW} (Hz) | $\log h_c$ |
|-----------|----------------|----------------|----------------------|------------|
| U Gem | 1.26 | 0.57 | $1.31 \cdot 10^{-4}$ | -20.8 |
| IP Peg | 1.15 | 0.67 | $1.46 \cdot 10^{-4}$ | -20.9 |
| HU Aqr | 0.95 | 0.15 | $2.67 \cdot 10^{-4}$ | -21.3 |
| VW Hyi | 0.63 | 0.11 | $3.12 \cdot 10^{-4}$ | -21.3 |
| EX Hya | 0.78 | 0.13 | $3.39 \cdot 10^{-4}$ | -21.4 |
| WZ Sge | 0.45 | 0.058 | $4.08 \cdot 10^{-4}$ | -22.1 |
| ST LMi | 0.76 | 0.17 | $2.93 \cdot 10^{-4}$ | -21.4 |
| SW UMa | 0.71 | 0.10 | $4.93 \cdot 10^{-4}$ | -21.6 |
| Z Cha | 0.84 | 0.125 | $3.11 \cdot 10^{-4}$ | -21.5 |
| V 436 Cen | 0.7 | 0.17 | $3.70 \cdot 10^{-4}$ | -21.6 |

masses, emission frequencies and characteristic wave amplitude are listed for some of these short period systems; among the systems analyzed in ref. 11, we have selected only those that emit gravitational waves large enough to be detectable by LISA with one year of integration.

4 Extrasolar planetary systems

In recent years a large number of extrasolar planetary systems have been discovered at very short distance from us¹², which exhibit some very interesting properties. They are very close to Earth (less than 10-20 pc), and they are formed by a solar type star and one or more orbiting companions, which can be planets, super-planets or, in some cases, brown dwarfs. Many of these companions are orbiting the main star at such short distance that conflicts with the predictions of the standard theories of planetary formation and evolution. For instance, some planets^b have orbital periods shorter than three days (for comparison, Mercury’s period is 88 days). In the light of these findings, it is interesting to ask the following question: is it possible that a planet orbit the main star so close as to excite one of its modes of oscillations? How much energy would be emitted in the form of gravitational waves by a system in this resonant condition, compared to the energy emitted because of the orbital motion? For how long would this condition persist? These questions have been analysed in two recent paper^{9 13}, whose results I shall briefly summarize. First of all we computed the frequencies of pulsation of the modes of a solar type

^bHere and in the following we shall indicate as “planet” also brown dwarfs and super planets.

Table 2: Values of the frequencies (in μHz) of the fundamental and of the first g-modes of oscillation of a solar-mass polytropic star with $n = 3$, for $\ell = 2$.

| | f-mode | g_1 | g_2 | g_3 | g_4 | g_5 | g_6 | g_7 | g_8 | g_9 | g_{10} |
|---------|--------|-------|-------|-------|-------|-------|-------|-------|-------|-------|----------|
| ν_i | 285 | 221 | 168 | 135 | 113 | 97 | 85 | 75 | 68 | 62 | 57 |

star, by integrating the equation of stellar perturbations in the framework of General Relativity. We considered a polytropic model of star, $p = K\epsilon^{1+1/n}$ with $n = 3$, adiabatic exponent $\gamma = 5/3$, central density $\epsilon_0 = 76 \text{ g/cm}^3$, and $c^2\epsilon_0/p_0 = 5.53 \cdot 10^5$. This model gives a star with the same mass and radius as the Sun¹³. In table 2 the values of the frequencies of the fundamental mode and of the first g-modes of the star are tabulated for $\ell = 2$. We do not include the frequencies of the p-modes because they are irrelevant to the following discussion.

If a planet moves on an orbit of radius R (we shall assume for simplicity that the orbit is circular), the keplerian orbital frequency is $\nu_k = \frac{1}{2\pi} \sqrt{\frac{G(M_\star + M_p)}{R^3}}$, where M_\star and M_p are the mass of the star and of the planet, respectively. The planet can excite a mode of frequency ν_i , only if ν_i is a specific multiple of the orbital frequency, i.e.

$$\nu_i = \ell \nu_k, \quad (5)$$

where ℓ is the considered multipole. Introducing the dimensionless frequency

$$k_i = \nu_i / \sqrt{\frac{GM_\star}{R_\star^3}},$$

where R_\star is the radius of the star, the resonant condition (5) can be written as

$$R_i = \left[\frac{\ell^2}{k_i^2} \cdot \left(1 + \frac{M_p}{M_\star} \right) \right]^{1/3} R_\star. \quad (6)$$

Thus, R_i is the value of the orbital radius for a given mode to be excited; for instance, using Eq. (6) we find that in order to excite the fundamental mode of the considered star, the planet should move on an orbit of radius smaller than 2 stellar radii, therefore we first need to verify whether a planet can move on such close orbit without being disrupted by the tidal interaction. This is equivalent to establish at which distance the star starts to accrete matter from

the planet (or viceversa), i.e. when the planet or the star overflow their Roche lobes ^c.

It is an easy exercise to compute the radius of the Roche lobe, R_{RL} , in newtonian theory, which fully applies to the case we are examining. If we choose a reference frame co-rotating with the two masses, with origin on the center of mass and such that the x-y plane coincides with the orbital plane, and the x-axis joins the two masses, the newtonian potential of the star-planet system can be written as

$$U(x, y) = -\frac{GM_p}{|\mathbf{x} - \mathbf{x}_p|} - \frac{GM_\star}{|\mathbf{x} - \mathbf{x}_\star|} - \frac{1}{2}\omega_k^2|\mathbf{x}|^2,$$

where $x_\star = \left(\frac{M_p}{M_p+M_\star}R, 0\right)$, $x_p = \left(-\frac{M_\star}{M_p+M_\star}R, 0\right)$, R is the orbital radius of the planet, and the last term is the centrifugal potential. A gas particle at a large radius on the planet may feel a gravitational force from the star that is comparable to, or even larger, than that from the planet. In that case, the gas particle is unstable against being transferred from the planet to the star. This can be understood by plotting contours of equal gravitational potential: if the potential is large and negative, the equipotential surfaces are two spheroids, one centered on M_p , the other on M_\star . As the potential increases the spheroids deform, and finally touch in one point lying on the axis which joins the star and the planet; the surface they form in this configuration is the Roche lobe surface, the unique point where the potential energy contour intersects itself is called the inner Lagrange point, and the curve which encloses the Roche lobes is said “first Lagrangian curve”. If the planet expands to fill its Roche lobe, the matter near the inner Lagrange point will spill over onto the star. Similarly, if the star fills its own Roche lobe it can accrete matter onto the planet. We can define the Roche lobe radius for the planet, R_{RL} , as the radius of the circle centered on the planet and tangent to the first Lagrangian curve (similarly for the star). R_{RL} can be found numerically, and it depends exclusively on the planet orbital radius R and on the star and planet masses.

The procedure to establish if a planet is allowed to orbit at a given distance from the star exciting its modes is the following:

- we assign a value of $R = R_i$ which corresponds to the excitation of a given mode, according to Eq. (6);
- we determine the Roche lobe radius $R_{RL}(R_i, M_p, M_\star)$ and compute the di-

^cFollowing the analysis in ref. ¹⁴, temperature effects, which may provoque the melting of the planet or the evaporation of its atmosphere, can be shown to be less stringent than the Roche-lobe limit.

Table 3: The critical ratio $\frac{\rho_{RL}}{\rho_\star}$ is given for three planets with mass equal to that of the Earth (M_E), of Jupiter (M_J) and of a brown dwarf with $M_{BD} = 40 M_J$, and for the different modes. This critical ratio corresponds to the minimum mean density that a planet should have in order to be allowed to move on an orbit which corresponds to the excitation of a g-mode, without being disrupted by tidal interactions.

| | $\frac{\rho_{RL}}{\rho_\star}$ | | | | | | | | | |
|----------|--------------------------------|-------|-------|-------|-------|-------|-------|-------|-------|----------|
| | g_1 | g_2 | g_3 | g_4 | g_5 | g_6 | g_7 | g_8 | g_9 | g_{10} |
| M_E | 12.5 | 7.21 | 4.64 | 3.24 | 2.38 | 1.83 | 1.45 | 1.17 | 0.97 | 0.82 |
| M_J | 13.0 | 7.49 | 4.82 | 3.37 | 2.48 | 1.90 | 1.51 | 1.22 | 1.01 | 0.85 |
| M_{BD} | - | - | - | 3.68 | 2.71 | 2.08 | 1.65 | 1.34 | 1.11 | 0.93 |

mensionless quantity \bar{R}_{RL} given by

$$\bar{R}_{RL} = R_{RL}/R_i; \quad (7)$$

- if the planet radius would be equal to R_{RL} , its average density would have a critical value, ρ_{RL} , given by

$$\rho_{RL} = \frac{M_p}{\frac{4}{3}\pi R_{RL}^3}. \quad (8)$$

Thus, if $\rho_p > \rho_{RL}$ the planet will not fill its Roche lobe and will not accrete matter on the star. Using Eqs. Eqs. (8),(6) and (7), the value of the critical density can be rewritten as

$$\rho_{RL} = \frac{M_p}{\frac{4}{3}\pi R_\star^3 \left[\frac{\ell^2}{k_i^2} \cdot \left(1 + \frac{M_p}{M_\star} \right) \right] \bar{R}_{RL}^3}, \quad (9)$$

or, normalizing to the mass of the central star, ρ_\star ,

$$\frac{\rho_{RL}}{\rho_\star} = k_i^2 \cdot \frac{M_p/M_\star}{\ell^2 (1 + M_p/M_\star) \bar{R}_{RL}^3}. \quad (10)$$

In conclusion, a planet can excite the i th-mode of the star without overflowing its Roche lobe, only if the ratio between its mean density and that of the central star is larger than the critical ratio (10).

We have computed the critical ratio (10) assuming that the central star has three different companion: two planets with the mass of the Earth and of Jupiter, and a brown dwarf of 40 jovian masses, M_E , M_J and M_{BD} , respectively, imposing that they are on an orbit which corresponds to the resonant

excitation of a given mode of the solar type star. We do not consider smaller planets because they produce gravitational signals that are too small to be interesting. The results of this analysis are shown in Table 3, where we tabulate the value of $\frac{\rho_{BD}}{\rho_*}$ for the three considered companions.

A planet like the Earth has a mean density such that $\rho_{Earth}/\rho_\odot = 3.9$, whereas for a planet like Jupiter $\rho_J/\rho_\odot = 0.9$; thus, from Table 3 we see that an Earth-like planet can orbit sufficiently close to the star to excite g-modes of order higher or equal to $n = 4$, whereas a Jupiter-like planet can excite only the mode g_{10} or higher. We find that in no case the fundamental mode can be excited without the planet being disrupted by accretion. According to the brown dwarf model (“model G”) by Burrows and Liebert¹⁵ an evolved, $40 M_J$ brown dwarf has a radius $R_{BD} = 5.9 \cdot 10^4$ km, and a corresponding mean density $\rho_{BD} = 88 \text{ g}\cdot\text{cm}^{-3}$; consequently $\rho_{BD}/\rho_\odot = 64$, and this value is high enough to allow a brown dwarf companion to excite all the g-modes of the central star. However, we also need to take into account the destabilizing mechanism of mass accretion *from* the central star. This imposes a further constraint, and this is the reason why the slots corresponding to the excitation of the g-modes lower than g_4 in the last row of Table 3 are empty.

Having established that some g-modes of the central star can, in principle, be excited, we turn to the next question, i.e. : how much energy would be emitted in gravitational waves by a system in this resonant condition, compared to the energy emitted because of the orbital motion? The amplitude of the wave emitted because of the orbital motion can be computed by using the quadrupole formula (1); in the case of circular orbit the characteristic amplitude (4) becomes

$$h_Q(R_i) = \frac{4M_p}{r} \sqrt{\frac{2}{15}} (\omega_k R_i)^2. \quad (11)$$

The values of this amplitude for the three planets considered above, are shown in table 4. However, if the stellar modes are excited the star will pulsate and emit more gravitational energy than that which can be computed by the quadrupole formula. In order to evaluate the resonant contribution we need to follow a different approach which takes into account the internal structure of the main star. One possibility is to use a perturbative approach which consists in the following. The main star is assumed to be an extended body, whose equilibrium structure is described by an exact solution of the relativistic equations of hydrostatic equilibrium; the planet is considered as a pointlike mass which induces a perturbation on the gravitational field and on the thermodynamical structure of the star. Under these assumptions we solve the equations of stellar perturbations to compute the characteristic amplitude of the gravitational

Table 4: The amplitude of the gravitational signal emitted when the three companions considered in Table 3 move on a circular orbit of radius R_i , such that the condition of resonant excitation of a g-mode is satisfied, is computed by the quadrupole formalism (see Eq. (11)) for the modes allowed by the Roche-lobe analysis. The planetary systems are assumed to be at a distance of 10 pc from Earth.

| | g_4 | g_5 | g_6 | g_7 | g_8 | g_9 | g_{10} |
|----------------------------------|-------|-------|-------|-------|-------|-------|----------|
| $h_Q^{Earth} \cdot 10^{26}$ | 3.0 | 2.7 | 2.5 | 2.3 | 2.2 | 2.0 | 1.9 |
| $h_Q^{BrownDwarf} \cdot 10^{22}$ | 3.9 | 3.5 | 3.2 | 3.0 | 2.8 | 2.6 | 2.4 |
| $h_Q^{Jupiter} \cdot 10^{24}$ | - | - | - | - | - | - | 6.1 |

wave emitted when the planet moves on a circular orbit close to a resonance¹³. In the following, we shall call this amplitude h_R , to indicate that it has been computed by solving the relativistic equations of stellar perturbations.

We have computed h_R for $\ell = 2$ (which is the relevant contribution), assuming that the planet moves on a circular orbit of radius $R_0 = R_i + \Delta R$, where R_i is the radius corresponding to the resonant excitation of the mode g_i , for the modes allowed by the Roche lobe analysis. We find that, as the planet approaches the resonant orbit, h_R grows very sharply. In figure 2 we plot the ratio $h_R(R_0)/h_Q(R_i)$ as a function of ΔR , to see how much the amplitude of the emitted wave increases, due to the excitation of a g-mode, with respect to the quadrupole emission. The plot is done for the modes g_4 , g_7 , and g_{10} , and it shows a power-law behaviour nearly independent of the order of the mode. It should be stressed that $h_R(R_0)/h_Q(R_i)$ is independent of the mass of the planet, but depends on the selected stellar model. From figure 2 we see that as the planet approaches a resonant orbit the amplitude of the emitted wave may become significantly higher than that computed by the quadrupole formalism, h_Q . Thus the next question to answer is how long can a planet orbit near a resonance, before radiation reaction effects move it off. Indeed, the loss of energy in gravitational waves causes a shrinking of the orbit of a planetary system, and the efficiency of this process increases as the planet approaches a resonant orbit. We shall now compute the time a planet takes to move from an orbit of radius $R_0 = R_i + \Delta R$, where the amplification factor h_R/h_Q has some assigned value, to the resonant orbit R_i , because of radiation reaction effects. This timescale will indicate whether a planet can stay in the resonant region long enough to be possibly observed. On the assumption that the timescale over which the orbital radius evolves is much longer than the orbital period

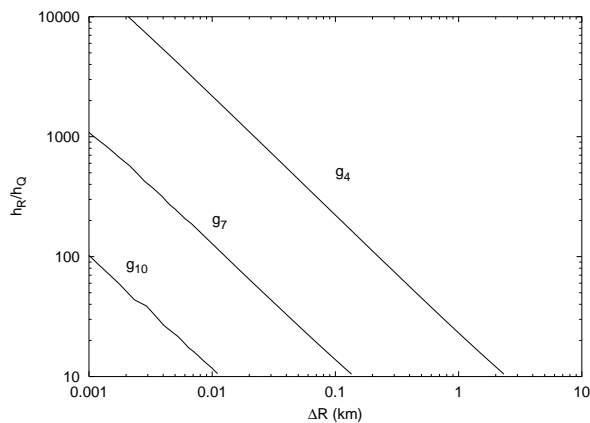


Figure 2: The logarithm of the ratio $h_R^{l=2}(R_i + \Delta R)/h_Q(R_i)$ is plotted as a function of ΔR for the modes g_4 , g_7 , and g_{10} .

(adiabatic approximation), the orbital shrinking can be computed from the energy conservation law

$$M_p \left\langle \frac{dE}{dt} \right\rangle + \left\langle \frac{dE_{GW}}{dt} \right\rangle = 0, \quad (12)$$

where E is the energy per unit mass of the planet which moves on the geodesic of radius R_0

$$E = \left(1 - \frac{2M_\star}{R_0} \right) \left(1 - \frac{3M_\star}{R_0} \right)^{-1/2}, \quad (13)$$

and $\left\langle \frac{dE_{GW}}{dt} \right\rangle$ is the energy emitted in gravitational waves, computed numerically by using the perturbative approach (see ref. ¹³ for details). Since $\left\langle \frac{dE}{dt} \right\rangle = \left\langle \frac{dR_0}{dt} \right\rangle / \left\langle \frac{dE}{dR_0} \right\rangle$, using Eq. (13) Eq. (12) gives

$$\left\langle \frac{dR_0}{dt} \right\rangle = - \frac{2R_0^2 (1 - 3M_\star/R_0)^{3/2}}{M_p M_\star (1 - 6M_\star/R_0)} \left\langle \frac{dE_{GW}}{dt} \right\rangle, \quad (14)$$

from which the time needed for the planet to reach the resonant orbit can be computed

$$\Delta T = - \frac{M_p M_\star}{2} \int_{R_i + \Delta R}^{R_i} \frac{(1 - 6M_\star/R_0)}{(1 - 3M_\star/R_0)^{3/2}} \frac{dR_0}{R_0^2 \left\langle \frac{dE_{GW}}{dt} \right\rangle}. \quad (15)$$

It should be noted that since $\langle \frac{dE_{GW}}{dt} \rangle$ is proportional to M_p^2 , ΔT is longer for smaller planets. We have computed ΔT for the three companions M_E , M_J and M_{BD} ,^d by the following steps:

- we assign a value of the orbital radius $R = R_i$ which corresponds to the excitation of a g-mode allowed by the Roche lobe analysis
- we compute the radius of the orbit $R_0 = R_i + \Delta R$ for which the amplification factor $A = h_R(R_0)/h_Q(R_i)$ has an assigned value
- we compute the energy radiated in gravitational waves, $\langle \frac{dE_{GW}}{dt} \rangle$, as a function of the orbital radius, in the range between R_0 and R_i
- using Eq. (15) we compute ΔT , which tells us how long can the planet orbit the star in the resonant region between R_0 and R_i , emitting a wave of amplitude higher than $[A \times h_Q(R_i)]$.

The results are summarized in table 5. These data have to be used together with those in table 4 as follows. Consider for instance a planet like the Earth, orbiting its sun on an orbit resonant with the mode g_4 . According to the quadrupole formalism it would emit a signal of amplitude $h_Q(R_4) = 3 \cdot 10^{-26}$, (table 4, first row) at a frequency $\nu_{GW} = 1.13 \cdot 10^{-4}$ Hz (table 5, first row). The data of table 5, which include the resonant contribution to the emitted radiation, indicate that before reaching that resonant orbit of radius R_4 , the Earth-like planet would orbit in a region of thickness $\Delta R = 1.7$ km slowly spiralling in, emitting waves with amplitude $h_R > 10h_Q(R_4) = 3 \cdot 10^{-25}$, for a time interval of $5.4 \cdot 10^6$ years, and that while spanning the smaller radial region $\Delta R = 312$ m, the emitted wave would reach an amplitude $h_R > 50h_Q(R_4) = 1.5 \cdot 10^{-24}$, for a time interval of $3.8 \cdot 10^4$ years. A jovian planet, on the other hand, could only excite modes of order $n = 10$ or higher, which would correspond to a resonant frequency of $\nu_{GW} = 5.7 \cdot 10^{-5}$ Hz and a gravitational wave amplitude greater than $6 \cdot 10^{-23}$ for 310 years ($\Delta R = 8$ m), or greater than $3 \cdot 10^{-22}$ for ~ 2 years ($\Delta R = 1$ m). From these data we see that the higher the order of the mode, the more difficult it is to excite it, because the region where the resonant effects become significant gets narrower and the planet transits through it for a shorter time. Much more interesting are the data for a brown dwarf companion. In this case, for instance, the region that would correspond to the resonant excitation of the mode g_4 ($\Delta R = 1.7$ km), with a wave amplitude greater than $3.9 \cdot 10^{-21}$, would be spanned in 430 years, whereas the emitted wave would have an amplitude greater than $\sim 2 \cdot 10^{-20}$ ($\Delta R = 312$ m) over a time interval of ~ 3 years. The results of this study show that if a brown dwarf would orbit a solar type star at such distance that

^d The data in table 5 have been obtained by repeating the calculations described in ref. ¹³, after correcting an error found in the numerical code. The qualitative results of ref. ¹³ are, however, correct.

Table 5: For each mode allowed by the Roche lobe analysis (see text), we give the frequency of the wave emitted when a planet moves on an orbit resonant with a g-mode of its sun (column 2). When the planet spans a radial region of thickness ΔR (column 3) approaching a resonant orbit, due to the stellar pulsations the amplitude of the emitted wave is amplified, with respect to the quadrupole amplitude, by a factor greater than A (column 4). In the last three columns we give the time interval ΔT needed for the three companions to span the region ΔR and reach the resonance.

| Mode | ν_{GW} (μHz) | ΔR (m) | A | ΔT_E (yrs) | ΔT_{BD} (yrs) | ΔT_J (yrs) |
|-----------------|-------------------------------|----------------|-----|--------------------|-----------------------|--------------------|
| g ₄ | 113 | 1700 | 10 | $5.4 \cdot 10^6$ | $4.3 \cdot 10^2$ | - |
| | | 312 | 50 | $3.8 \cdot 10^4$ | 3.0 | - |
| g ₅ | 97 | 616 | 10 | $2.7 \cdot 10^6$ | $2.1 \cdot 10^2$ | - |
| | | 113 | 50 | $1.9 \cdot 10^4$ | 1.5 | - |
| g ₆ | 85 | 240 | 10 | $1.4 \cdot 10^6$ | $1.1 \cdot 10^2$ | - |
| | | 44 | 50 | $9.6 \cdot 10^3$ | $7.5 \cdot 10^{-1}$ | - |
| g ₇ | 75 | 98 | 10 | $7.0 \cdot 10^5$ | 55 | - |
| | | 18 | 50 | $5.0 \cdot 10^3$ | $3.9 \cdot 10^{-1}$ | - |
| g ₈ | 68 | 42 | 10 | $3.8 \cdot 10^5$ | 30 | - |
| | | 8 | 50 | $2.5 \cdot 10^3$ | $1.9 \cdot 10^{-1}$ | - |
| g ₉ | 62 | 18 | 10 | $1.9 \cdot 10^5$ | 15 | - |
| | | 3 | 50 | $1.5 \cdot 10^3$ | $1.2 \cdot 10^{-1}$ | - |
| g ₁₀ | 57 | 8 | 10 | $1.0 \cdot 10^5$ | 7.8 | $3.1 \cdot 10^2$ |
| | | 1 | 50 | $6.7 \cdot 10^2$ | $5.3 \cdot 10^{-2}$ | 2.1 |

a g-mode is excited, the emitted radiation may be strong enough, and for a sufficiently long time interval, to be detectable by LISA.

5 Coalescing binary systems

The main target of ground-based interferometers is to detect the signal emitted during the late phases of inspiraling of a binary system. Assuming that the two coalescing bodies are two point masses, M_1 and M_2 , by using the quadrupole formalism and including the radiation reaction effects (along the lines discussed in Sec. 4), it is possible to show that the loss of gravitational energy induces a circularization of the orbit¹⁶, and that the radius decreases according to the law $R(t) = R_{in} (1 - t/t_{coal})^{1/4}$; where $t_{coal} = \frac{5}{256} \frac{R_{in}^4}{\mu M^2}$ is the time of the final coalescence, and $\mu = M_1 M_2 / M$ is the reduced mass of the system of total mass $M = M_1 + M_2$. The orbital frequency consequently increases, and so does the frequency of the emitted wave, with a time dependence given

by $\nu = \frac{1}{\pi} \left[\frac{5}{256} \frac{1}{\mu M^{2/3}} \frac{1}{(t_{\text{coast}} - t)} \right]^{3/8}$. Thus, the gravitational signal emitted by a coalescing system resembles the chirp of a singing bird.

At some point of the evolution, for instance $\sim 10^8$ years after formation if the binary system is composed of two neutron stars, the frequency of the emitted signal enters the bandwidth of the ground based interferometers, and in about 15-20 minutes (depending on the mass of the stars) sweeps the frequency region ranging from $\sim 10\text{Hz}$ up to $\sim 900\text{Hz}$. The amplitudes of the two polarizations of the wave emitted during this fast inspiralling phase are

$$h_+ = \frac{2(1 + \cos^2 i)\mu(\pi M\nu)^{2/3}}{r} \cos(2\pi\nu t), \quad h_\times = \pm \frac{4\mu \cos i (\pi M\nu)^{2/3}}{r} \sin(2\pi\nu t), \quad (16)$$

where i is the angle of inclination of the orbit to the line of sight, and the emitted energy per unit frequency is given by $\frac{dE}{d\nu} = \frac{\pi^{2/3}}{3} \mu \frac{M^{2/3}}{\nu^{1/3}}$.

This description of the coalescence based on the quadrupole formalism breaks down when the two stars are so close that tidal effects become important. For instance, for binaries with one white dwarf companion, the maximum frequency, i.e. the minimum distance between the two stellar components, is set in order to cut-off the Roche-lobe contact stage. In fact, the mass transfer from one component to its companion transforms the original detached binary into a semi-detached binary. This process can be accompanied by loss of angular momentum with mass loss from the system and the above description cannot be applied. In this case, the minimum orbital separation that two white dwarfs can reach is given by $r_{wd}(M_1) + r_{wd}(M_2)$, where $r_{wd}(M) = 0.012R_\odot \sqrt{(M/1.44M_\odot)^{-2/3} - (M/1.44M_\odot)^{2/3}}$ is the approximate formula for the radius of a white dwarf¹⁷. If the system is composed, say, by two white dwarfs of $0.9 M_\odot$, the cutoff frequency is $\nu_{GW \text{ max}} \sim 0.1 \text{ Hz}$. These signals are therefore candidates for detection by spaceborne interferometers.

The situation is different for NS-binaries or BH-binaries because, being the two bodies extremely compact, the pointlike approximation described above works remarkably well up to much higher frequencies, where the post-newtonian formalism can be applied to correct the waveforms emitted during the latest phases of the inspiral; however, even this more refined waveforms fail to correctly reproduce the emitted signal when the innermost stable circular orbit (ISCO) is approached, particularly when the coalescing bodies are neutron stars. Indeed, in a recent paper we have shown that due to a resonant excitation of the modes of oscillation of the stars, the emitted energy may be enhanced with respect to the orbital contribution¹⁸. This phenomenon emerges only if we use an approach in which the stars are allowed to have an internal

Table 6: Parameters of the polytropic stars we consider in our analysis: the polytropic index n , the central density, the ratio $\alpha_0 = c^2 \epsilon_0 / p_0$ of central density to central pressure, the mass, the radius and the ratio R/M (in geometric units). The central density is chosen in such a way that the stellar mass is equal to $1.4M_\odot$, except for model A, the mass of which is about one solar mass.

| Model number | n | ϵ_0 (g/cm ³) | α_0 | M (M_\odot) | R (km) | R/M |
|--------------|-----|-----------------------------------|------------|-------------------|----------|-------|
| A | 1.5 | 1.00×10^{15} | 13.552 | 0.945 | 14.07 | 10.08 |
| B | 1 | 6.584×10^{14} | 9.669 | 1.4 | 15.00 | 7.26 |
| C | 1.5 | 1.260×10^{15} | 8.205 | 1.4 | 15.00 | 7.26 |
| D | 1 | 2.455×10^{15} | 4.490 | 1.4 | 9.80 | 4.74 |
| E | 1.5 | 8.156×10^{15} | 2.146 | 1.4 | 9.00 | 4.35 |

structure, which plays a dynamical role by exchanging energy with the gravitational field. For instance, in¹⁸ we have used the same perturbative approach described in Sec. 4 to study the emission of extrasolar planetary systems: we assume that one of the two neutron is a “true” neutron star, whose equilibrium structure is governed by the TOV equations of hydrostatic equilibrium, whereas the second star is a point mass which perturbs the gravitational field and the fluid of the extended companion. To extract the effects that the internal structure of the star has on the gravitational emission we have selected a set of parameters which allow to encompass a reasonable range of stellar models, and to cover most of the range of structural properties obtained with realistic EOS. The values of the parameters are given in Table 6. For each model, we have integrated the equations of stellar perturbations in General Relativity, and we have computed the energy flux emitted in gravitational waves, \dot{E}^R , assuming that the perturbing point mass, m_0 , is moving on a circular orbit of radius R_0 , with orbital velocity v , and semilatus rectum p , given by

$$v = (M\omega_k)^{1/3} = \frac{1}{\sqrt{p}}, \quad (17)$$

where M is the mass of the star. The results are shown in Fig. 3, where we plot the normalized energy flux, $P \equiv \dot{E}^R / \dot{E}^N$, where \dot{E}^N is the orbital contribution computed by the quadrupole formalism

$$\dot{E}^N = \frac{32}{5} \frac{m_0^2}{M^2} v^{10}. \quad (18)$$

$P(v)$ has been obtained by adding the contributions of different l and m , with $2 \leq l \leq 7$, and it is plotted in Fig. 3 as a function of the orbital velocity,

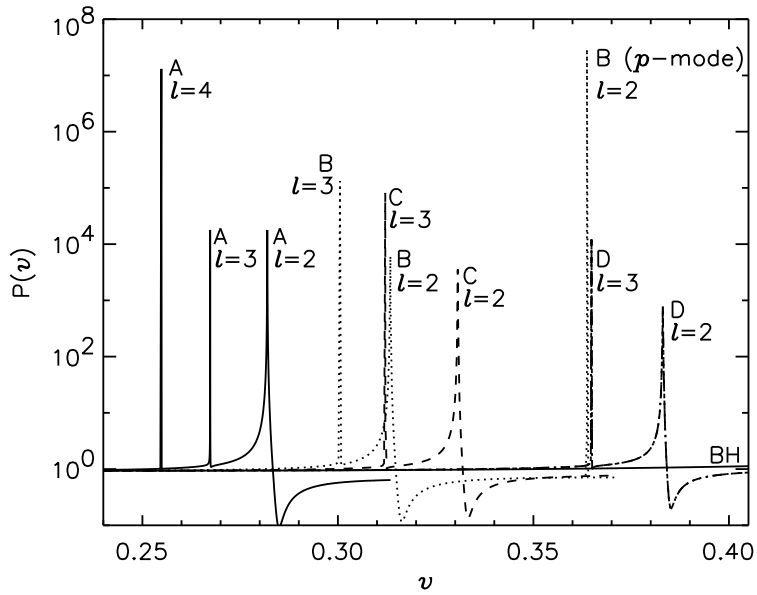


Figure 3: The normalized energy flux, $P(v)$, is plotted as a function of the orbital velocity for the stellar models given in Table 6 and for a black hole. For model D and for the black hole the curves extend up to the velocity which correspond to the ISCO, whereas for the other models they stop when the mass m_0 reaches the surface of the star. The sharp peaks indicate that, for different values of the harmonic index l , the fundamental quasi-normal modes of the star are excited if the orbital frequency satisfies the resonant condition (5); the curve of the stellar model B has a peak at high v which correspond to the excitation of the first p-mode for $l = 2$. The most compact model E is not shown in the figure because at this scale it is indistinguishable from the black hole.

for the models of star we have considered; for comparison, we also plot $P(v)$ computed in the case when the perturbed object is a black hole. In this case the plot extends up to the velocity which corresponds to the ISCO, $R_0 = 6M$, whereas for the stellar models it stops when m_0 reaches the surface of the star. From Fig. 3 we see that sharp peaks appear if the central object is a star: they correspond to the excitation of the fundamental quasi-normal modes of the star for different values of the harmonic index ℓ . In the case of model B the first p-mode for $\ell = 2$ is also excited. Since the peaks of the mode excitation are very high, the scale chosen on the vertical axis of Fig. 3 makes the response of the black hole to appear as a flat line. The reason is that, since the frequency of the lowest quasi-normal modes of a black hole are much higher than those of a star with the same mass, the circular orbit that would excite them would have a radius smaller than $6M_{BH}$. Thus, in the range of v considered in Fig. 3 the energy flux emitted by the black hole is due essentially to the orbital motion. In Fig. 4, we show a zoom of Fig. 3 restricted to the region $v < 0.28$, which is far enough from the resonant orbits (except that for model A). In this case we can appreciate the differences between the emission of different stellar models and that of a black hole. If the orbital velocity is smaller than 0.16 all curves are practically indistinguishable. Fig. 4 shows that the normalized energy fluxes emitted by different stellar models have a different slope, and are always larger than the flux emitted by the black hole. The increase in the energy output at orbital velocities larger than $v = 0.16$ is just an effect of the resonance tail.

6 Concluding Remarks

In this review we have shown how to estimate the characteristic features of the gravitational signals emitted by some interesting astrophysical sources.

Chances to detect these waves crucially depend on the detailed knowledge of the waveform; indeed the standard technique used to extract a non-continuous signal from the noisy data of a detector is the matched filtering technique, whose performances are very sensitive to a mismatching of the parameters: for this reason the templates must be as accurate as possible. Since the most interesting signals are emitted in spacetime regions where the non linearity of the gravitational interaction plays an important role, the ultimate template would be that obtained by integrating the fully non linear equations of General Relativity. However, fully nonlinear simulations of phenomena like the gravitational collapse or the coalescence of binary systems are, at present, at a preliminary stage, although major progresses in the field are underway. Thus, for the time being we need to rely on the results obtained by approxi-

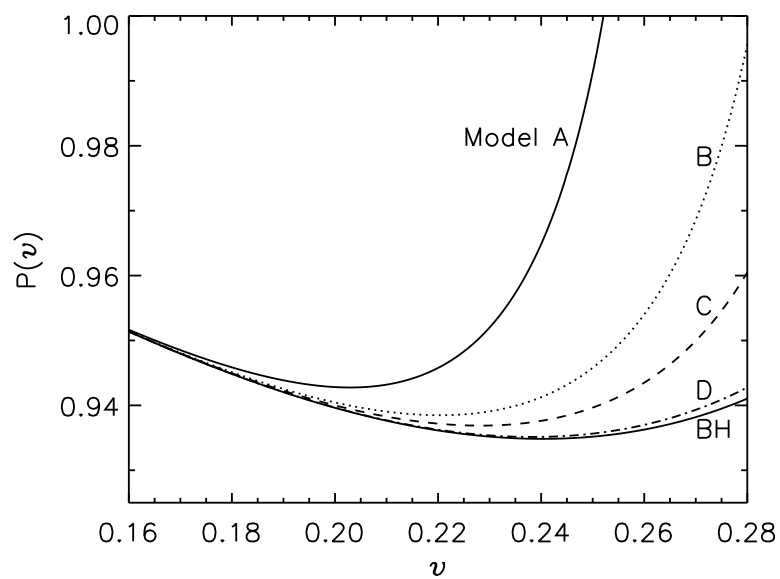


Figure 4: The normalized energy flux, $P(v)$, is plotted as in Fig. 1, but for a smaller orbital velocity range, such that the peaks due to the excitation of the stellar modes are excluded.

mate methods, like the quadrupole formalisms and the perturbative approach, to mention those we have described in this paper. There are many things that we learn from these approaches. Consider for instance the evolution of a binary system: the quadrupole formalism, applied to point masses, allows to determine with high accuracy the gravitational signal emitted when the two bodies are far apart, the frequencies and the expected amplitudes. Including radiation reaction effects and using the adiabatic approximation, we can predict how the orbit evolves, and how much time it takes to become circular. However, if the system is composed by a solar type star and a close planet (or a brown dwarf companion), new phenomena may occur, like the resonant excitation of the g-modes of the star, which can be accounted for only if the internal structure of the star is included in the picture; in this case, the perturbative approach provides the tools needed to evaluate how much energy is radiated in gravitational waves because of the stellar oscillations, at which frequencies, and for how long can a system be in a resonant condition.

If the binary system is formed by very compact objects, like neutron stars or black holes, the quadrupole approach works up to much higher frequencies, since in this case the masses can really be treated, to a large extent, as point masses. During the latest phases of the inspiralling, let say during the 10-20 cycles that precede the merging when the signal frequency is of the order of 900-1000 Hz, the non linearity of the interaction produces deviations from the quadrupole signal which can be estimated by introducing post-newtonian corrections at higher order of (v/c) (see e.g. ¹⁹ and references quoted there). In the standard post-newtonian (PN) approach, the coalescing bodies are still considered as point masses, and this is good enough for black holes. However, in the case of NS-binaries the fundamental mode of the stars may be excited in the same region, and this excitation may produce corrections to the quadrupole signal that are comparable or higher than the PN corrections, and depend on the internal structure of the stars; as we have shown in Sec. 5, these phenomena can be studied again by a perturbative approach, which has been shown to work remarkably well, even when the two stars are at a distance as short as three stellar radii ¹⁸.

An accurate detection of the signal emitted during the last few cycles before coalescence may enlighten unresolved issues related to the internal composition of neutron stars and to the state of matter at supernuclear density. These effects, however will not be seen by the first generation of interferometers, for which the most likely source to be detected is the coalescence of BH-BH binaries with masses of the order of $20 - 30 M_{\odot}$ ²⁰. But there is hope for the future: advanced detectors are being proposed like EURO, a european project now under a feasibility study, that should be extremely sensitive at

high frequency, and would allow to study the processes we have described.

Acknowledgments

The work on relativistic stellar perturbations described in this lecture has been supported by the EU Programme 'Improving the Human Research Potential and the Socio-Economic Knowledge Base' (Research Training Network Contract HPRN-CT-2000-00137).

References

1. For details of the interferometric experiments see the web sites: virgo.infn.it, ligo.caltech.edu, geo600.uni-hannover.de, tamago.ntk.nao.ac.jp, lisa.jpl.nasa.gov
2. P.Astone, *Class. Quant. Grav.* to appear
3. R.A. Hulse, J.H. Taylor, *Astrophys. J.* **195**, L51 (1975).
4. S.Bonazzola, E. Gourgoulhon, *Astron. Astrophys.* **312**, 675 (1996).
5. E. Gourgoulhon, S. Bonazzola, *Proceedings of the International Conference on Gravitational Waves, Sources and Detectors*, World Scientific, Singapore 1996, 51
6. G. Ushomirsky, C. Cutler, L. Bildsten, *Mon. Not. R. Astron. Soc.* to appear (2000), astro-ph/0001136.
7. R. Smoluchowski, *Phys. Rev. L.* **24**, 923 (1970).
8. R. Ruderman, *Ap. J.* **382**, 587 (1991).
9. V. Ferrari, M. D'Andrea, E. Berti, *Int. J. Mod. Phys. D* **9 n. 5**, 495 (2000)
10. K.S. Thorne, *300 Years of Gravitation*, ed. S. Hawking and W. Israel, Cambridge University Press, 1987, 330.
11. M. T. Meliani, J.C.N. de Araujo and O.D. Aguiar, *A & A* **358**, 417 (2000)
12. For an updated catalogue of new extrasolar planetary systems see the web sites: <http://exoplanets.org/almanacframe.html>
13. E. Berti, V. Ferrari, *Phys. Rev. D* **63**, 064031 (2001).
14. T. Guillot, A. Burrows, W.B.Hubbard, J.I. Lunine and D. Saumon, *Ap. J* **459**, L35 (1996).
15. A. Burrows, J. Liebert, *Rev. Mod. Phys.* **65**, 301 (1993)
16. P.C. Peters, J. Mathews, *Phys. Rev.* **131**, 435 (1963)
17. M. Nauenberg, *Astrophys. J.* **175**, 417 (1972)
18. J.A. Pons, L. Gualtieri, E. Berti, G. Miniutti, V. Ferrari, submitted to *Phys Rev D* (2001), [gr-qc/0111104](http://arxiv.org/abs/gr-qc/0111104)

19. T. Damour, B. R. Iyer, B. S. Sathyaprakash, *Phys. Rev. D* **57**, 885 (1998)
20. L.P. Grishchuk, V.M. Lipunov, K.A. Postnov, M.E. Prokhorov, B.S. Sathyaprakash, *Phys.Usp.* **44**, 1 (2001)
21. For information on the third generations Gravitational wave observatory, see the web site: <http://www.astro.cf.ac.uk/geo/euro/>